A FRAME RECONSTRUCTION ALGORITHM WITH APPLICATIONS TO MAGNETIC RESONANCE IMAGING

JOHN J. BENEDETTO[1], ALFREDO NAVA-TUDELA[2], ALEXANDER M. POWELL[3], AND YANG WANG[4]

Abstract. A frame theoretic technique is introduced that combines Fourier and finite frames. The technique is based on fundamental theorems by Beurling and Landau in the theory of Fourier frames, and transitions to the finite frame case, where an algorithm is constructed. The algorithm exhibits the strengths of frame theory dealing with noise reduction and stable signal reconstruction. It was designed to resolve problems dealing with fast spectral data acquisition in magnetic resonance imaging (MRI), and has applicability to a larger class of signal reconstruction problems.

1. Introduction

1.1. **Background.** We introduce a combined Fourier and finite frame technique to resolve a class of signal reconstruction problems, where efficient noise reduction and stable signal reconstruction are essential. This class includes the special case of obtaining fast spectral data acquisition in magnetic resonance imaging (MRI) [32]. Fast data acquisition is important for a variety of reasons. For example, human subject motion during the MRI process should be analyzed by methods that do not blur essential features, and speed of data acquisition lessens the effect of such motion. We shall use the MRI case as a prototype to explain our idea. Generally, our approach includes the transition from a theoretically conclusive reconstruction method using Fourier frames to a finite frame algorithm designed for effective computation.

Date: November 28, 2016.

2010 *Mathematics Subject Classification.* 42C15, 65F.

Key words and phrases. Magnetic resonance imaging, frame theory, computational algorithm, transpose reduction, stability .

The first named author gratefully acknowledges the support of ARO Grant W911NF-15-1-0112, DTRA Grant 1-13-1-0015, and ARO Grant W911NF-16-1-0008. The second named author gratefully acknowledges the support of the Norbert Wiener Center and the Institute for Physical Science and Technology. The third named author gratefully acknowledges the support of NSF DMS Grant 1521749, as well as the hospitality and support of the Academia Sinica Institute of Mathematics (Taipei, Taiwan). The fourth named author gratefully acknowledges the support of the Hong Kong Research Grant Council, Grants 16306415 and 16317416, as well as of AFOSR Grant FA9550-12-1-0455. All of the authors appreciate the world class expertise of Prof. Niranjan Ramachandran of the University of Maryland, College Park, of Dr. Richard Spencer of NIH, and of Prof. David F. Walnut of George Mason University, and their generosity in sharing with us. In the case of Prof. Ramachandran, his number theoretic insights were particularly important; in the case of Dr. Spencer, his deep knowledge of NMR and MRI was vital; and, in the case of Prof. Walnut, his scholarship and technical skills dealing with uniform distribution and the discrepancy of sequences was comparably essential. Also, the first named author thanks Hui-Chuan Wu, whose exceptional talent is matched by her wonderful humanity. It was with her in the 1990s that he began his journey in this subject in terms of classical harmonic analysis. Finally, the authors acknowledge the useful comments and constructive suggestions of the two referees, all of which has been incorporated into this final version.

To begin, the use of interleaving spirals in the spectral domain, so-called k–space when dealing with MRI, is one viable setting for attaining fast MRI signal reconstruction in the spatial domain; and a major method in this regard is spiral–scan echo planar imaging (SEPI), e.g., see [23]. With this in mind, the Fourier frame component of our technique goes back to results of Beurling [13] and Henry J. Landau [42], as well as a reformulation of the Beurling–Landau theory in the late 1990s that was made with Hui-Chuan Wu, see [11], [10], [12]. This reformulation is in terms of quantitative coverings of a spectral domain by translates of the polar set of the target/subject disk space D in the spatial domain. In this context, harmonics for Fourier frames can be constructed by means of the Beurling–Landau theory on interleaving spirals in the spectral domain, allowing for the reconstruction of signals in D.

The finite frame component of our technique was developed in 2002, when the four co-authors worked together, see [6].

There has been major progress with regard to MRI and fMRI, *and* the importance of effective SEPI has *not* been diminished.

With regard to the progress, MRI and fMRI are often essentially effected in real–time [22], and technologies such as wavelet theory [33], compressed sensing [45], and non-uniform FFTs [25], [26], [30], [37] have also been used to advantage.

Although SEPI is faster than conventional rectilinear sampling, the fastest rectilinear echo planar imaging (EPI), which can be faster than SEPI, is prone to artifacts from gradient switching which is often ameliorated in SEPI. Further, SEPI is still of potential great importance with regard to spectroscopic imaging [2] and fMRI, e.g., dynamic imaging of blood flow [50].

Amidst all of this complexity, a distinct advantage of frame oriented techniques, such as ours, is the potential for effective noise reduction and stable signal reconstruction in the MRI process. With regard to frames, noise reduction, and stable reconstruction, we refer to [8], [5], and see [38], [39] for an authoritative more up to date review. The point is that noise reduction can be effected by modeling in which information bearing signals can be moved into a coefficient subspace relatively disjoint from coefficients representing noise in the system. This idea has a long history in the engineering community, and the theory of frames provides an excellent model to effect such a transformation. In fact, frames that are not bases allow one to construct Bessel mappings, see Section 3, that are not surjective, giving rise to the aforementioned subspaces; and the the overcompleteness inherent in frames guarantees stable signal representation, e.g., see [20] and [4], Chapter 7.

1.2. **Outline.** Section 2 describes spiral–scan echo planar imaging (SEPI), beginning with the imaging equation for MR in which the NMR (nuclear magnetic resonance) signal $S(t)$ is obtained by integrating the solution of Bloch's differential equation. The phenomenon of NMR was discovered independently by Felix Bloch and Edward Purcell, see [18], page 13, for historical comments (the word nuclear gives the false impression that nuclear material is used). Section 7 expands on this material by means of a sequence of images with brief explanations.

Section 3 provides the mathematical background for our theory and algorithm. This includes the theory of frames and a fundamental condition for the existence of Fourier frames due to Beurling and Landau. We also have an alternative parallel approach depending on a multidimensional version of Kadec's sufficient condition for Riesz bases in the Fourier frame case. In Section 4, we first describe our algorithm conventionally and, keeping in mind our interest in noise reduction and stable reconstruction, we then formulate it in frame theoretic terms. This allows us to prove a basic theorem on computational stability (Theorem 3) indicating the importance of designing frames that are tight or, at least, almost tight. Naturally, our algorithm, which is discrete, should also have the theoretical property that, in the limit, it will be a constructive way of genuinely approximating analogue images, whose discrete versions are computed by the algorithm. This is the content of Section 5.

Section 6 is devoted to refinements of the formulation in Section 4 in order to effect useful implementation.

Finally, after Section 7 we close with Section 8, that outlines the paradigm we have used to manufacture data in which to evaluate our algorithm when MRI generated data is not available.

2. An MRI problem

A standard MRI equation is a consequence of Felix Bloch's equation for transverse magnetization M_{tr} in the presence of a linear magnetic field gradient [18] pages 269-270, see Section 7. In fact, an MR signal $S(t)$ is the integration of M_{tr}; and the corresponding imaging equation is

$$S(t) = S(k(t)) = S(k_x(t), k_y(t), k_z(t)) \tag{1}$$

$$= \int\int\int \rho(x,y,z) \exp[-2\pi i \langle (x,y,z),\ (k_x(t),k_y(t),k_z(t))\rangle] e^{-t/T_2} dx\ dy\ dz,$$

e.g., see [17], [33], [18], pages 269-270, [14], Subsection 16.2, page 344. $S(t)$ is also referred to as an *echo* or *FID* (free induction decay), and can be measured for the sake of imaging. Equation (1) is a natural physical Fourier transform associated with magnetization, analagous to the natural physical wavelet transform effected by the behavior of the basilar membrane within certain frequency ranges, e.g., [7].

The parameters, variable, and inputs in Equation (1) are the following:

$$k_x(t) = \gamma \int_0^t G_x(u) du \tag{2}$$

and $G_x(u)$ is an x-directional time varying gradient with similar definitions for the y and z variables, T_2 is the transverse relaxation time, the exponential term e^{-t/T_2} representing the T_2 decay appears as a limiting factor in echo planar imaging [1], γ is the gyromagnetic ratio, and $\rho(\mathbf{r}) = \rho(x,y,z) = \rho(\mathbf{r}, T_2)$ is the spatial spin density distribution from which the spin density image is reconstructed.

Since $S(t)$ is a measurable quantity in the MR process and since precise knowledge of $\rho(x,y,z)$ is desired, it is natural to compute the inverse Fourier transform of S, properly adapted to the format in Equation (2). Because of significant issues which arise and goals which must be addressed, the inversion process has to be treated carefully. In particular, there is a significant role for the time-varying gradients. First, the gradients are inputs to the process, and must be designed theoretically in order to be realizable and goal oriented. Once the gradients have been constructed, the imaging data $S(t)$ at time t is really of the form $S(k(t))$ as seen in Equations (1) and (2); and it is usual to refer to the *spectral* domain of S as k–space. See Section 7 for more detail for this process.

Example 1. Let

$$G_x(t) = \eta \cos \xi t - \eta \xi t \sin \xi t$$

and

$$G_y(t) = \eta \sin \xi t + \eta \xi t \cos \xi t.$$

By the definition of k_x, k_y, see Equation (2), we compute $k_x(t) = \gamma \eta t \cos \xi t$ and $k_y(t) = \gamma \eta t \sin \xi t$. Combining k_x and k_y we obtain the Archimedean spiral,

$$A_c = \{(c\theta \cos 2\pi\theta, c\theta \sin 2\pi\theta) : \theta \geq 0\} \subseteq \widehat{\mathbb{R}}^2,$$

where γ, η, and $\xi > 0$ are considered as constants, $\theta = \theta(t) = (1/2\pi)\,\xi t$, and $c = 2\pi\gamma\eta/\xi$. Clearly, we have $\theta(t) \to \infty$ as $t \to \infty$.This idea for formulating time domain gradient pulse forms is due to Ljunggren [44]. They clearly generate a spiral scan in the k–domain and are not difficult to realize, see Figure 1.

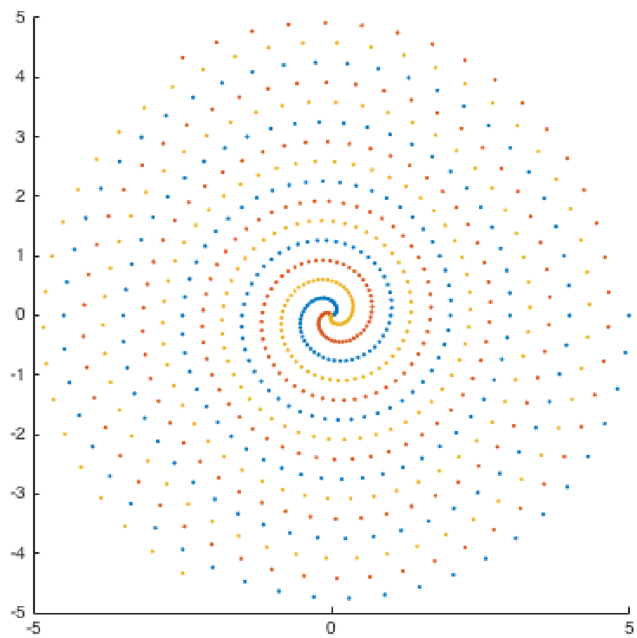

FIGURE 1. Archimedean sampling example with three Archimedean spirals in the k domain.

Remark 1. *a.* The echo planar imaging (EPI) method, developed by Mansfield (1977) [18], page 306, theoretically and usually provides high speed data acquisition within the time interval of a few hundreths of seconds. The method utilizes multiple echos by fast gradient alternation. As such, realizable gradient design giving rise to large high speed gradient fields is essential. A solution to this design problem has to be coupled with controlling spatial resolution limits imposed by the T_2-decay in Equation (1), e.g., [18] pages 314-315.

A weakness of this technique as originally formulated is that the alternating gradient to be applied is a series of rectangular pulses which are difficult to generate for high gradient power and frequency, see [1], pages 2-3, for this and a fuller critique.

b. SEPI ensures rapid scanning for fast data acquisition. Spiral scanning also simplifies the scanning of data in radial directions once the span is completed. In this regard the inherent T_2 effect appears as an almost circular blurring which is preferable to the one-dimensional blurs observed in earlier EPI. Further, there is a reduction in transient and steady state distortion, since SEPI eliminates the discontinuities of gradient waveforms which arise in uniform rectilinear scanning that proceeds linearly around corners while transversing k-space, e.g., [1], [18].

Interleaving spiraling from rapid spiral scans proceeds from dc levels to high frequencies. That such multiple pulsing can be implemented in SEPI is due to its locally circular symmetry property in data acquisition, and the resulting interleaving spirals yield high resolution imaging when accompanied by effective k–space sampling and reconstruction methods, see [35]. In fact, interleaving spiral scans not only improve k-space sampling strategies, but they also overcome the gradient requirement and T_2-decay limitations for standard EPI.

c. EPI and SEPI are both fast in terms of image data acquisition, but the off resonance and flow properties of the two methods differ; and, in fact, total scan time spiral imaging requires lower gradient power than EPI, e.g., [43]. Further, SEPI has more significantly reduced artifact intensities than the 2–dimensional FFT since its spiral trajectories collect low spatial frequencies with every view; and it also seems to be superior vis-à-vis motion insensitivity, see [29], [28].

3. Fourier frames and Beurling's theorem

3.1. **Frames and Beurling's theorem.**

Definition 1. *a.* Let H be a separable Hilbert space. A sequence $\{x_n : n \in \mathbb{Z}^d\} \subseteq H$ is a *frame* for H if there exist constants $0 < A \leq B < \infty$ such that

$$\forall y \in H, \quad A\|y\|^2 \leq \sum |\langle y, x_n\rangle|^2 \leq B\|y\|^2.$$

The optimal constants, viz., the supremum over all such A and infimum over all such B, are called the *lower* and *upper frame bounds* respectively. When we refer to *frame bounds* A and B, we shall mean these optimal constants.

b. A frame X for H is a *tight frame* if $A = B$. If a tight frame has the further property that $A = B = 1$, then the frame is a *Parseval frame* for H.

c. A frame X for H is *equal-norm* if each of the elements of X has the same norm. Further, a frame X for H is a *unit norm tight frame* (UNTF) if each of the elements of X has norm 1. If H is finite dimensional and X is an UNTF for H, then X is a *finite unit norm tight frame* (*FUNTF*).

d. A sequence of elements of H satisfying an upper frame bound, such as $B\|x\|^2$ in part a, is a *Bessel sequence.*

There is an extensive literature on frames, e.g., see [24], [52], [20], [9], [4], [19], [15].

Let $X = \{x_j\}$ be a frame for H. We define the following operators associated with every frame. They are crucial to frame theory. The *analysis operator* $L : H \to \ell^2(\mathbb{Z}^d)$ is defined by

$$\forall x \in H. \quad Lx = \{\langle x, x_n\rangle\}.$$

The second inequality of Definition 1, part a, ensures that the analysis operator L is bounded. If H_1 and H_2 are separable Hilbert spaces and if $T : H_1 \to H_2$ is a linear operator, then the *operator norm* $\|T\|_{op}$ of T is

$$\|T\|_{op} = \sup_{\|x\|_{H_1} \leq 1} \|T(x)\|_{H_2}.$$

Clearly, we have $\|L\|_{op} \le \sqrt{B}$. The adjoint of the analysis operator is the *synthesis operator* $L^* : \ell^2(\mathbb{Z}^d) \to H$, and it is defined by

$$\forall a \in \ell^2(\mathbb{Z}^d), \quad L^* a = \sum_{n\in\mathbb{Z}^d} a_n x_n.$$

From Hilbert space theory, we know that any bounded linear operator $T : H \to H$ satisfies $\|T\|_{op} = \|T^*\|_{op}$. Therefore, the synthesis operator L^* is bounded and $\|L^*\|_{op} \le \sqrt{B}$.

The *frame operator* is the mapping $S : H \to H$ defined as $S = L^*L$, i.e.,

$$\forall x \in H, \quad Sx = \sum_{n\in\mathbb{Z}^d} \langle x, x_n \rangle x_n.$$

We shall describe S more fully. First, we have that

$$\forall x \in H, \quad \langle Sx, x \rangle = \sum_{n\in\mathbb{Z}^d} |\langle x, x_n \rangle|^2 .$$

Thus, S is a positive and self-adjoint operator, and the inequalities of Definition 1, part a, can be rewritten as

$$\forall x \in H, \quad A\|x\|^2 \le \langle Sx, x\rangle \le B\|x\|^2 ,$$

or, more compactly, as

$$AI \le S \le BI.$$

It follows that S is invertible ([20], [4]), S is a multiple of the identity precisely when X is a tight frame, and

$$B^{-1}I \le S^{-1} \le A^{-1}I. \tag{3}$$

Hence, S^{-1} is a positive self-adjoint operator and has a square root $S^{-1/2}$ (Theorem 12.33 in [48]). This square root can be written as a power series in S^{-1}; consequently, it commutes with every operator that commutes with S^{-1}, and, in particular, with S. Utilizing these facts we can prove a theorem that tells us that frames share an important property with orthonormal bases, viz., there is a reconstruction formula [9], Theorem 3.2.

Theorem 1 (Frame reconstruction formula)**.** *Let H be a separable Hilbert space, and let $X = \{x_n\}_{n\in\mathbb{Z}^d}$ be a frame for H with frame operator S. Then,*

$$\forall x \in H, \quad x = \sum_{n\in\mathbb{Z}^d} \langle x, x_n \rangle S^{-1}x_n = \sum_{n\in\mathbb{Z}^d} \left\langle x, S^{-1}x_n \right\rangle x_n = \sum_{n\in\mathbb{Z}^d} \left\langle x, S^{-1/2}x_n \right\rangle S^{-1/2}x_n.$$

Proof. The proof is three computations. From $I = S^{-1}S$, we have

$$\forall x \in H, \quad x = S^{-1}Sx = S^{-1}\sum_{n\in\mathbb{Z}^d} \langle x, x_n \rangle x_n = \sum_{n\in\mathbb{Z}^d} \langle x, x_n \rangle S^{-1}x_n;$$

from $I = SS^{-1}$, we have

$$\forall x \in H, \quad x = SS^{-1}x = \sum_{n\in\mathbb{Z}^d} \left\langle S^{-1}x, x_n \right\rangle x_n = \sum_{n\in\mathbb{Z}^d} \left\langle x, S^{-1}x_n \right\rangle x_n;$$

and from $I = S^{-1/2}SS^{-1/2}$, it follows that

$$\forall x \in H,\ x = S^{-1/2}SS^{-1/2}x = S^{-1/2}\sum_{n\in\mathbb{Z}^d} \left\langle S^{-1/2}x, x_n \right\rangle x_n = \sum_{n\in\mathbb{Z}^d} \left\langle x, S^{-1/2}x_n \right\rangle S^{-1/2}x_n. \quad \square$$

Let $\mathbb{R}^d$ be d-dimensional Euclidean space, and let $\widehat{\mathbb{R}}^d$ denote $\mathbb{R}^d$ when it is considered as the domain of the Fourier transforms of signals defined on $\mathbb{R}^d$. The Fourier transform of $f : \mathbb{R}^d \longrightarrow \mathbb{C}$ is formally defined as

$$\varphi(\gamma) = \widehat{f}(\gamma) = \int_{\mathbb{R}^d} f(x)\, e^{-2\pi i x\cdot\gamma}\, dx.$$

The *Paley-Wiener* space PW_D is

$$PW_D = \left\{ \varphi \in L^2(\widehat{\mathbb{R}}^d) : \operatorname{supp} \varphi^\vee \subseteq D \right\},$$

where $D \subseteq \mathbb{R}^d$ is closed, $L^2(\widehat{\mathbb{R}}^d)$ is the space of finite energy signals φ on $\widehat{\mathbb{R}}^d$, i.e.,

$$\|\varphi\|_{L^2(\widehat{\mathbb{R}}^d)} = \left(\int_{\widehat{\mathbb{R}}^d} |\varphi(\gamma)|^2\, d\gamma \right)^{1/2} < \infty,$$

$\varphi^\vee$ is the inverse Fourier transform of φ defined as

$$\varphi^\vee(x) = \int_{\widehat{\mathbb{R}}^d} \varphi(\gamma) e^{2\pi i x\cdot\gamma} d\gamma,$$

and $\operatorname{supp} \varphi^\vee$ denotes the support of $\varphi^\vee$.

Notationally, let $e_\lambda(x) = e^{2\pi i x\cdot\lambda}$, where $x \in \mathbb{R}^d$ and $\lambda \in \widehat{\mathbb{R}}^d$.

Definition 2. Let $\Lambda \subseteq \widehat{\mathbb{R}}^d$ be a sequence, and let $D \subseteq \mathbb{R}^d$ be a closed set having finite Lebesgue measure. It is elementary to see that $\mathcal{E}(\Lambda) = \{e_{-\lambda} : \lambda \in \Lambda\}$ is a frame for the Hilbert space $L^2(D)$ if and only if there exist $0 < A \le B < \infty$ such that

$$\forall \varphi \in PW_D, \quad A\|\varphi\|^2_{L^2(\widehat{\mathbb{R}}^d)} \le \sum_{\lambda\in\Lambda} |\varphi(\lambda)|^2 \le B\|\varphi\|^2_{L^2(\widehat{\mathbb{R}}^d)}.$$

In this case, and because of this equivalence, we say that Λ is a *Fourier frame* for PW_D.

It is elementary to verify the following equivalence.

Proposition 1. $\mathcal{E}(\Lambda) = \{e_{-\lambda} : \lambda \in \Lambda\}$ *is a frame for the Hilbert space* $L^2(D)$ *if and only if the sequence,*

$$\{\widehat{(e_{-\lambda}\mathbb{1}_D)} : \lambda \in \Lambda\} \subseteq PW_D,$$

is a frame for PW_D*, in which case it is also called a* Fourier frame *for* PW_D.

Recall that a set Λ is *uniformly discrete* if there is $r > 0$ such that

$$\forall \lambda, \gamma \in \Lambda, \quad |\lambda - \gamma| \ge r,$$

where $|\lambda - \gamma|$ is the Euclidean distance between λ and γ.

Beurling [13] proved the following theorem for the case that D is the closed ball $B(0, R) \subseteq \mathbb{R}^d$ centered at $0 \in \mathbb{R}^d$ and with radius R.

Theorem 2. *Let* $\Lambda \subseteq \widehat{\mathbb{R}}^d$ *be uniformly discrete, and define*

$$\rho = \rho(\Lambda) = \sup_{\zeta\in\widehat{\mathbb{R}}^d} \operatorname{dist}(\zeta, \Lambda),$$

where $\operatorname{dist}(\zeta, \Lambda) = \inf\{|\zeta - \lambda| : \lambda \in \Lambda\}$. *If* $R\rho < 1/4$, *then* Λ *is a Fourier frame for* $PW_{B(0,R)}$.

By the definition of Fourier frame the assertion of Beurling's theorem is that every finite energy signal f defined on D has the representation,

$$f(x) = \sum_{\lambda \in \Lambda} a_\lambda(f) e^{2\pi i x \cdot \lambda}, \tag{4}$$

in L^2-norm on D, where $\sum_{\lambda\in\Lambda} |a_\lambda(f)|^2 < \infty$. Beurling [13] and [42] used the term *set of sampling* instead of *Fourier frame*. In practice, signal representations such as Equation (4) often undergo an additional quantization step to achieve analog-to-digital conversion of the signal, e.g., [47].

In theory, for the case $D = B(0, R)$, we can not expect to construct either tight or exact Fourier frames for the spiral in Subsection 3.2, see [27].

It is possible to make a quantitative comparison between Kadec's 1/4-theorem and Theorem 2. For now we provide the following remark which shows that the construction of Subsection 3.2 can also be achieved by use of Kadec's theorem.

Remark 2. Kadec (1964) [36] proved that *if* $\Lambda = \{\lambda_m : m \in \mathbb{Z}\} \subseteq \widehat{\mathbb{R}}$ *and* $\sup_{m\in\mathbb{Z}} |\lambda_m - \frac{m}{2R}| < 1/4$, *then* Λ *is a Riesz basis for* $PW_{[-R,R]}$. This means that $\{e^{2\pi i\lambda_m/R}\}$ is an exact frame for $PW_{[-R,R]}$, which, in turn, means it is a bounded unconditional basis for $PW_{[-R,R]}$ or, equivalently, that it is a frame which ceases to be a frame if any of its elements is removed, see, e.g., [52].

3.2. **Fourier frames on interleaving spirals.** We can now address the problem of imaging speed in the data acquisition process of MRI in terms of the imaging equation, Equation (1), translated into a Fourier frame decomposition. In fact, $\lambda \in \Lambda \subseteq \widehat{\mathbb{R}}^2$ in Equation (4) corresponds to $(k_x(t), k_y(t), k_z(t))$ in Equation (1) in the case $k_z(t)$ is identically 0.

We use Theorem 2 to give a constructive non-uniform sampling signal reconstruction method in the setting of spirals and their interleaves. The method is much more general than the geometry of interleaving spirals.

For the case of spirals there are three cases: given an Archimedean spiral A, to show there is $R > 0$, generally small, and a Fourier frame $\Lambda \subseteq A$ for $PW_{B(0,R)}$ (the calculation for this case uses techniques from the following case); given an Archimedean spiral A and $R > 0$, to show there are finitely many interleaves of A and a Fourier frame Λ, contained in their union, for $PW_{B(0,R)}$ (Example 2); given $R > 0$, to show there is an Archimedean spiral A and a Fourier frame $\Lambda \subseteq A$ for $PW_{B(0,R)}$ (Example 3).

Example 2. *a.* Given *any* $R > 0$ and $c > 0$. Notationally, we write any given $\xi_0 \in \widehat{\mathbb{R}}^2$ as $\xi_0 = r_0 e^{2\pi i\theta_0} \in \mathbb{C}$, where $r_0 \geq 0$ and $\theta_0 \in [0, 1)$. We shall show how to construct a finite interleaving set $B = \cup_{k=1}^{M-1} A_k$ of spirals,

$$A_k = \left\{c\theta e^{2\pi i(\theta - k/M)} : \theta \geq 0\right\}, \quad k = 0, 1, \ldots, M-1,$$

and a uniformly discrete set $\Lambda_R \subseteq B$ such that Λ_R is a Fourier frame for $PW_{B(0,R)}$. Thus, all of the elements of $L^2(B(0, R))$ will have a decomposition in terms of the Fourier frame $\{e_\lambda : \lambda \in \Lambda_R\}$, see [11], [10], [12] for the original details.

b. We begin by choosing M such that $cR/M < 1/2$. Then, either $0 \leq r_0 < c\theta_0 < c$ or there is $n_0 \in \mathbb{N} \cup \{0\}$ for which

$$c(n_0 + \theta_0) \leq r_0 < c(n_0 + 1 + \theta_0).$$

In this latter case, we can find $k \in \{0, \dots, M-1\}$ such that

$$c(n_0 + \theta_0 + \frac{k}{M}) \le r_0 < c(n_0 + \theta_0 + \frac{k+1}{M}).$$

Thus,

$$\operatorname{dist}(\xi_0, B) \le \frac{c}{2M}.$$

Next, we choose $\delta > 0$ such that $R\rho < 1/4$, where $\rho = (c/2M + \delta)$.

Then, for each $k = 0, 1, \dots, M-1$, we choose a uniformly discrete set Λ_k of points along the spiral A_k having curve distance between consecutive points less than 2δ, and beginning within 2δ of the origin. The curve distance, and consequently the ordinary distance, from any point on the spiral A_k to Λ_k is less than δ. Finally, we set $\Lambda_R = \cup_{k=0}^{M-1} \Lambda_k$. Thus, by the triangle inequality, we have

$$\begin{aligned} \forall \xi \in \widehat{\mathbb{R}}^2, \quad \operatorname{dist}(\xi, \Lambda_R) &\le \operatorname{dist}(\xi, B) + \operatorname{dist}(B, \Lambda_R) \\ &\le \frac{c}{2M} + \delta = \rho, \end{aligned}$$

where $\operatorname{dist}(B, \Lambda_R) = \inf \{|\zeta - \lambda| : \zeta \in B \,\text{and}\, \lambda \in \Lambda_R\}$. Hence, $R\rho < 1/4$ by our choice of M and δ; and so we invoke Beurling's theorem, Theorem 2, to conclude that Λ_R is a Fourier frame for $PW_{B(0,R)}$.

Example 3. Note that since we are reconstructing signals on a space domain having area about R^2, we require essentially R interleaving spirals. On the other hand, if we are allowed to choose the spiral(s) after we are given $PW_{B(0,R)}$, then we can choose Λ_R contained in a *single* spiral A_c for $c > 0$ small enough.

Remark 3. *a.* There have been refinements and generalizations of Kadec's theorem (Remark 2), that are relevant to our approach, e.g., Sun and Zhou [51]. In fact, given $R > 0$, the Sun and Zhou result gives rise to exact frames for $L^2([-R, R]^d)$ which become frames for $L^2(B(0, R))$. For $d = 2$, the corresponding set $\Lambda \subseteq \widehat{\mathbb{R}}^2$ can be chosen on interleaves of a given spiral $A \subseteq \widehat{\mathbb{R}}^2$. This allows us to replace the application of Beurling's theorem in Examples 2 and 3 by a multi-dimensional Kadec theorem.

b. It can be proved that it is not possible to cover a separable lattice by finitely many interleaves of an Archimedean spiral, see [46]. In particular, sampling for the spiral MRI problem can not be accomplished by simply overlaying spirals on top of a lattice, and then appealing to classical sampling theory on lattices. Consequently, it is a theoretical necessity that non-uniform sampling results, such as the Beurling's or Kadec's theorem, are required in the spiral case.

4. The transition to finite frames

4.1. **Algorithm.** Let $D = [0, 1)^2$ and let $N > 1$. The space $L^2_N(D)$ of N-*digital images* is the closed subspace of $L^2(D)$ consisting of all piecewise constant functions, $f \in L^2(D)$, of the form

$$f(x, y) = f_{k,l} \quad \text{for } (x, y) \in \left[\frac{k}{N}, \frac{k+1}{N}\right) \times \left[\frac{l}{N}, \frac{l+1}{N}\right), \; 0 \le k, l < N.$$

We use the notation, $\alpha = (\lambda, \mu) \in \widehat{\mathbb{R}}^2$ and $e(s) = e^{-2\pi i s}$, $s \in \mathbb{R}$. For a given $f \in L^2_N(D)$, we compute

$$\widehat{f}(\alpha) = -\frac{1}{4\pi^2 \lambda\mu} \sum_{k,l=0}^{N-1} f_{k,l} \cdot e\left(\frac{k\lambda + l\mu}{N}\right) \left[e\left(\frac{\lambda}{N}\right) - 1\right] \left[e\left(\frac{\mu}{N}\right) - 1\right].$$

Setting

$$G_{k,l}(\lambda, \mu) = e\left(\frac{k\lambda + l\mu}{N}\right) \left[e\left(\frac{\lambda}{N}\right) - 1\right] \left[e\left(\frac{\mu}{N}\right) - 1\right],$$

we have

$$\widehat{f}(\alpha) = \widehat{f}(\lambda, \mu) = -\frac{1}{4\pi^2 \lambda\mu} \sum_{k,l=0}^{N-1} f_{k,l} G_{k,l}(\lambda, \mu). \tag{5}$$

Since there are N^2 unknowns, $f_{k,l}$, if we have N^2 or more samples of $\widehat{f}(\alpha)$, say $\{\widehat{f}(\alpha_m)\}_{m=0}^{M-1}$ with $M \geq N^2$, where $\Lambda = \{\alpha_m\}_{m=0}^{M-1}$ is properly chosen in the square $\left[-\frac{N}{2}, \frac{N}{2}\right]^2$, then we have a necessary condition for being able to reconstruct $\{f_{k,l}\}$. In fact, we suppose that the following *conditions* are satisfied.

(1) $M \geq N^2$, and, in fact, we may want sufficient over-sampling so we may choose $M \gg N^2$, e.g., $M \approx 4N^2$.
(2) The periodic extension $\Lambda + K\mathbb{Z}^2$ gives rise to a frame $\mathcal{E}(\Lambda + K\mathbb{Z}^2)$ for $L^2_N(D)$ with frame constants A, B, see Proposition 1. This can be proved for Λ constructed in the square $\left[-\frac{N}{2}, \frac{N}{2}\right)^2$. In the case of SEPI for MRI imagery, this is achieved by taking $\{\alpha_m\}$ on a few tightly wound spirals.

We shall show that the samples $\Lambda = \{\alpha_m\}_{m=0}^{M-1}$ allow us to reconstruct f in a stable manner. We begin by writing

$$H_{k,l}(\lambda, \mu) = -\frac{1}{4\pi^2 \lambda\mu} G_{k,l}(\lambda, \mu). \tag{6}$$

Hence, by (5), we have

$$\widehat{f}(\lambda, \mu) = \sum_{k,l=0}^{N-1} f_{k,l} H_{k,l}(\lambda, \mu). \tag{7}$$

Ordering $\{(k, l) : 0 \leq k, l < N\}$ lexicographically as $\{a_n : n = 0, \ldots, N^2 - 1\}$, we obtain

$$\widehat{f}(\lambda, \mu) = \sum_{n=0}^{N^2-1} f_{a_n} H_{a_n}(\lambda, \mu). \tag{8}$$

Therefore, we can write

$$\widehat{f}(\alpha_m) = \sum_{n=0}^{N^2-1} f_{a_n} H_{a_n}(\alpha_m). \tag{9}$$

We define the vectors,

$$\mathbb{F} = \begin{pmatrix} f_{a_0} \\ \vdots \\ f_{a_{N^2-1}} \end{pmatrix} \quad \text{and} \quad \widehat{\mathbb{F}} = \begin{pmatrix} \widehat{f}(\alpha_0) \\ \vdots \\ \widehat{f}(\alpha_{M-1}) \end{pmatrix},$$

and the matrix,

$$\mathbb{H} = (H_{a_n}(\alpha_m))_{m,n}\,. \tag{10}$$

It is convenient notationally to set $H_n = H_{a_n}$. and so $\mathbb{H}$ can be written as

$$\mathbb{H} = \begin{pmatrix} H_0(\alpha_0) & \dots & H_{N^2-1}(\alpha_0) \\ H_0(\alpha_1) & \dots & H_{N^2-1}(\alpha_1) \\ \vdots & & \vdots \\ H_0(\alpha_{M-1}) & \dots & H_{N^2-1}(\alpha_{M-1}) \end{pmatrix}. \tag{11}$$

We obtain

$$\widehat{\mathbb{F}} = \mathbb{H}\mathbb{F}. \tag{12}$$

Since (12) is an over-determined system, we find the least-square approximation, yielding

$$\mathbb{F} = (\mathbb{H}^*\mathbb{H})^{-1}\mathbb{H}^*\widehat{\mathbb{F}}, \tag{13}$$

where $\mathbb{H}^* = \overline{\mathbb{H}}^{\mathrm{T}}$ and T denotes the transpose operation, i.e., $*$ is the usual Hermitian involution for matrices. Note that $\mathbb{H}$ is an $M \times N^2$ matrix, and so $\mathbb{H}^*$ is an $N^2 \times M$ matrix and $\mathbb{H}^*\mathbb{H}$ is an $N^2 \times N^2$ matrix.

Equation (13) asserts that $\mathbb{F}$ is the Moore-Penrose pseudo-inverse of $\widehat{\mathbb{F}}$, and a major goal is to mold this equation into a viable algorithm and computational tool with regard to noise reduction and stable reconstruction, see Section 6. It should be pointed out that Moore-Penrose has played a role in the reconstruction of MR images, going back to Van de Walle et al. (2000) and Knutsson et al. (2002). However, unprocessed application of Moore-Penrose is not feasible for typical MR image sizes, as the work of Samsonov et al. and Fessler illustrates. In fact, our frame theoretic approach is meant to provide a new technique for experts in MRI to develop.

Equation (13) can be written in frame-theoretic terminology. In fact, $\mathbb{H}$ is the analysis operator $L : l^2(\{0, ...N^2 - 1\}) \to l^2(\{0, ...M - 1\})$, $\mathbb{H}^*$ is its adjoint synthesis operator L^*, and the frame operator $S = L^*L$ is $\mathbb{H}^*\mathbb{H}$. Defining the Gramian $R = LL^*$, we have

$$f = (S^{-1}L^*)Lf,$$

and

$$f = (L^*R^{-1})Lf,$$

where $f \in l^2(\{0, ...N^2 - 1\})$. Clearly, Equation (13) is $f = (S^{-1}L^*)Lf$ in our frame theoretic notation.

Remark 4. Define the space $F_N^2(D) \subseteq L^2(D)$ of *continuous N-digital images* as

$$F_N^2(D) = \left\{ \sum_{m=0}^{N-1}\sum_{n=0}^{N-1} f_{m,n}\Delta\left(x - \frac{m}{N}, y - \frac{n}{N}\right) : \{f_{m,n}\}_{m,n=0}^{N-1} \subseteq \mathbb{R} \right\},$$

where $\Delta(x, y) = \Delta(x)\Delta(y) = \Delta^N(x)\Delta^N(y)$, and $\Delta^N(x)$ is the triangle function supported by $[0, 1/N]$ whose Fourier transform is the usual Fejér kernel. We introduce $F_N^2(D)$ in order to increase the speed of our algorithm, Equation (13). In fact, in forthcoming work we provide a Fejér kernel reconstruction algorithm with which to refine Equation (13).

4.2. **Computational Stability.** We must find out to what extent the reconstruction scheme of Section 4.1, in which we evaluate the coefficients $f_{k,\ell}$ in Equation (5), is stable. To this end,we would like to show that the condition number,

$$\kappa(\mathbb{H}^*\mathbb{H}) = \text{cond}(\mathbb{H}^*\mathbb{H}) = \frac{|\lambda_{\max}(\mathbb{H}^*\mathbb{H})|}{|\lambda_{\min}(\mathbb{H}^*\mathbb{H})|}, \tag{14}$$

is not too large, where $\lambda_{\max}$, $\lambda_{\min}$ denote the *maximum* and *minimum* eigenvalues of $\mathbb{H}^*\mathbb{H}$. Thus, the problem is precisely that such a reconstruction scheme is not necessarily stable because the matrix $\mathbb{H}^*\mathbb{H}$ may have a large condition number. Consequently, if the sampled values $\widehat{f}(\alpha)$ are noisy, the reconstruction may not be useful. This is where the theory of frames can be applied to yield a stable reconstruction.

We can check that that $\mathbb{H}^*\mathbb{H}$ is positive definite, and so the absolute values on the right side of Equation (14) can be omitted. Further, $\mathbb{H}^*\mathbb{H}$ is a normal operator (matrix).

The following theorem underlies a useful algorithmic approach, but *must* be made more precise in the sense that the *conditions* of Subsection 4.1 be made with more specificity.

Theorem 3. *Given* $\mathbb{H}$ *as defined in Equation* (10)*, and assume* $X = \Lambda + N\,\mathbb{Z}^2$ *is a Fourier frame for* $L^2(D)$ *with frame bounds* A *and* B*. Then,*

$$\text{cond}(\mathbb{H}^*\mathbb{H}) \leq \left(\frac{\pi}{2}\right)^4 \frac{B}{A}.$$

Proof. Let $\alpha = (\lambda, \mu) \in \Lambda + N\mathbb{Z}^2$. Then, $\alpha = \alpha_m + N\gamma$ for some $0 \leq m < M$ and $\gamma \in \mathbb{Z}^2$. Let $g \in L^2([0,1]^2)$ be an N-digital image, i.e.,

$$g(x,y) = g_{k,l} \quad \text{for } a = (x,y) \in \left[\frac{k}{N}, \frac{k+1}{N}\right) \times \left[\frac{l}{N}, \frac{l+1}{N}\right).$$

By (5), we compute

$$\begin{aligned}\widehat{g}(\alpha) &= \sum_{k,l=0}^{N-1} \int_{\frac{k}{N}}^{\frac{k+1}{N}} \int_{\frac{l}{N}}^{\frac{l+1}{N}} g_{k,l} e(a\cdot\alpha) da, \\ &= -\frac{1}{4\pi^2\lambda\mu} \sum_{k,l=0}^{N-1} g_{k,l} G_{k,l}(\alpha),\end{aligned}$$

where $\alpha = (\lambda, \mu)$ and $e(s) = e^{-2\pi i s}$, $s \in \mathbb{R}$. Let $\alpha_m = (\lambda_m, \mu_m) \in \Lambda$. Then,

$$\widehat{g}(\alpha) = -\frac{1}{4\pi^2\lambda\mu} \sum_{k,l=0}^{N-1} g_{k,l}\; G_{k,l}(\alpha_m), \tag{15}$$

$$= \frac{\lambda_m\mu_m}{\lambda\mu}\widehat{g}(\alpha_m).$$

Therefore, with $\gamma = (\gamma_x, \gamma_y)$, we compute

$$\begin{aligned}\sum_{\alpha \in \Lambda + N\mathbb{Z}^2} |\widehat{g}(\alpha)|^2 &= \sum_{m=0}^{M-1} \sum_{\gamma \in \mathbb{Z}^2} |\widehat{g}(\alpha_m + N\gamma)|^2 \\ &= \sum_{m=0}^{M-1} \sum_{\gamma \in \mathbb{Z}^2} \left(\frac{\lambda_m \mu_m}{(\lambda_m + N\gamma_x)(\mu_m + N\gamma_y)} \right)^2 |\widehat{g}(\alpha_m)|^2.\end{aligned}$$

It is easy to check that, since $(\lambda_m, \mu_m) = \alpha_m \in (-N/2, N/2)^2$, we have

$$\begin{aligned}1 \leq &\sum_{\gamma \in \mathbb{Z}^2} \left(\frac{\lambda_m \mu_m}{(\lambda_m + N\gamma_x)(\mu_m + N\gamma_y)} \right)^2 \\ = &\sum_{\gamma_x \in \mathbb{Z}} \left(\frac{\lambda_m}{\lambda_m + N\gamma_x} \right)^2 \cdot \sum_{\gamma_y \in \mathbb{Z}} \left(\frac{\mu_m}{\mu_m + N\gamma_y} \right)^2 \\ = &\frac{1}{\operatorname{sinc}^2(\frac{\pi \lambda_m}{N})} \cdot \frac{1}{\operatorname{sinc}^2(\frac{\pi \mu_m}{N})},\end{aligned}$$

where we use the identity,

$$\sum_{n \in \mathbb{Z}} \frac{t^2}{(t + Nn)^2} = \frac{1}{\operatorname{sinc}^2(\frac{\pi t}{N})},$$

with $\operatorname{sinc}(t) = \frac{\sin t}{t}$, see [34], Equation (10).

We know that

$$\frac{1}{\operatorname{sinc}^2(\frac{\pi \lambda_m}{N})} \frac{1}{\operatorname{sinc}^2(\frac{\pi \mu_m}{N})} \leq \left(\frac{\pi}{2} \right)^4.$$

Therefore, the fact that

$$\sum_{\alpha \in \Lambda + N\mathbb{Z}^2} |\widehat{g}(\alpha)|^2 = \sum_{m=0}^{M-1} \sum_{\gamma \in \mathbb{Z}^2} \left[\frac{\lambda_m \mu_m}{(\lambda_m + N\gamma_x)(\mu_m + N\gamma_y)} \right]^2 |\widehat{g}(\alpha_m)|^2$$

allows us to make the estimate,

$$\sum_{m=0}^{M-1} |\widehat{g}(\alpha_m)|^2 \leq \sum_{\alpha \in \Lambda + N\mathbb{Z}^2} |\widehat{g}(\alpha)|^2 \leq \left(\frac{\pi}{2} \right)^4 \sum_{m=0}^{M-1} |\widehat{g}(\alpha_m)|^2.$$

Hence, it follows from the inequalities,

$$A\|g\|_{\mathrm{L}^2}^2 \leq \sum_{\alpha \in \Lambda + N\mathbb{Z}^2} |\widehat{g}(\alpha)|^2 \leq B\|g\|_{\mathrm{L}^2}^2,$$

that

$$\left(\frac{2}{\pi} \right)^4 A\|g\|_{\mathrm{L}^2}^2 \leq \sum_{m=0}^{M-1} |\widehat{g}(\alpha_m)|^2 \leq B\|g\|_{\mathrm{L}^2}^2. \tag{16}$$

Now, replacing f with g in Equation (12), we obtain

$$\widehat{\mathbb{G}} = \mathbb{H}\,\mathbb{G}.$$

Therefore,

$$\mathbb{G}^*(\mathbb{H}^*\mathbb{H})\mathbb{G} = \widehat{\mathbb{G}}^*\widehat{\mathbb{G}} = \sum_{m=0}^{M-1} |\widehat{g}(\alpha_m)|^2. \tag{17}$$

Observe that

$$\|\mathbb{G}\|^2 = \sum_{k,l=0}^{N-1} |g_{k,l}|^2 = N^2\|g\|^2_{\mathrm{L}^2}.$$

Combining (16) and (17) leads to

$$\frac{(\frac{2}{\pi})^4 A}{N^2}\|\mathbb{G}\|^2 \leq \mathbb{G}^*(\mathbb{H}^*\mathbb{H})\mathbb{G} \leq \frac{B}{N^2}\|\mathbb{G}\|^2; \tag{18}$$

and so

$$\lambda_{\max}(\mathbb{H}^*\mathbb{H}) \leq \frac{B}{N^2},$$

and

$$\lambda_{\min}(\mathbb{H}^*\mathbb{H}) \geq \left(\frac{2}{\pi}\right)^4 \frac{A}{N^2}.$$

Hence, we conclude that

$$\operatorname{cond}(\mathbb{H}^*\mathbb{H}) \leq \left(\frac{\pi}{2}\right)^4 \frac{B}{A}.$$

□

5. Asymptotic properties of the algorithm

Given the samples $\{\widehat{f}(\alpha_j)\}_{j=0}^{M-1}$ and $N \in \mathbb{N}$, where $f \in L^2(D)$, $M > N^2$, and $\{\alpha_j\}_{j=0}^{M-1} \subseteq [-k/2, k/2] \times [-k/2, k/2] \subseteq \widehat{\mathbb{R}}^2$, the reconstruction $f_{\text{recon}} \in L^2_N(D)$, should serve as an approximation to f, see Equation (13). We quantify that wish in this subsection. We begin with the following, which is not difficult to verify.

Proposition 2. *Given $f \in L^2(D)$ and $N \in \mathbb{N}$. The function $g \in L^2_N(D)$, that minimizes $\|f - g\|_2$ is*

$$g(x,y) = \sum_{k,l=0}^{N-1} g_{k,l}\mathbb{1}_{[\frac{k}{N},\frac{k+1}{N})}(x)\mathbb{1}_{[\frac{l}{N},\frac{l+1}{N})}(y),$$

where

$$g_{k,l} = \frac{1}{\left|\left[\frac{k}{N},\frac{k+1}{N}\right) \times \left[\frac{l}{N},\frac{l+1}{N}\right)\right|}\int_{[\frac{k}{N},\frac{k+1}{N})\times[\frac{l}{N},\frac{l+1}{N})} f(x,y)\,dx\,dy,$$

i.e., $g_{k,l}$ is the average of f over $\left[\frac{k}{N},\frac{k+1}{N}\right) \times \left[\frac{l}{N},\frac{l+1}{N}\right)$.

From the definition of $H_{k,l}$ in Equation (6), we have

$$H_{k,l}(\lambda,\mu) = \widehat{\mathbb{1}}_{[\frac{k}{N},\frac{k+1}{N})}(\lambda)\widehat{\mathbb{1}}_{[\frac{l}{N},\frac{l+1}{N})}(\mu), \tag{19}$$

and, as in Subsection 4.1, recall that we order $\{(k,l) : 0 \leq k,l < N\}$ lexicographically as $\{a_n\}_{n=0}^{N^2-1}$. Also, let $D^N_{a_n}$ be the square, $\left[\frac{k}{N},\frac{k+1}{N}\right) \times \left[\frac{l}{N},\frac{l+1}{N}\right)$, where a_n is the lexicographic integer corresponding to the word (k,l). For convenience, we write $D_n = D^N_{a_n}$.

The asymptotic behavior of the algorithm is formulated in the following assertion. The mathematical calculation to verify this behavior follows the assertion, see Remark 5.

Asymptotic behavior of the algorithm. *Let $f \in L^2(D)$ and fix N. Assume $K \gg 0$ and assume $\{\alpha_j\}_{j=0}^{M-1}$ is essentially uniformly distributed* [40] *in the square, $\left[-\frac{K}{2}, \frac{K}{2}\right] \times \left[-\frac{K}{2}, \frac{K}{2}\right]$, as $M \to \infty$. Then, for $M \gg 0$, we obtain the approximation,*

$$\forall n = 1, \ldots, N^2 - 1, \quad f_{a_n} \approx \frac{1}{|D_n|} \int_{D_n} f(x,y)dxdy, \tag{20}$$

where $|D_n| = 1/N^2$ is the area of D_n, and where the f_{a_n} are the coefficients of f_{recon} for a given element of $L_N^2(D)$. Thus, comparing Equation (20) *with Proposition 2, we see that, as $M \to \infty$, the algorithm reconstruction, f_{recon}, approaches the optimal $L_N^2(D)$ approximation of f.*

Note that

$$\mathbb{H}^*\mathbb{H} = \begin{pmatrix} c_{0,0} & \cdots & c_{0,N^2-1} \\ \vdots & & \vdots \\ c_{N^2-1,0} & \cdots & c_{N^2-1,N^2-1} \end{pmatrix},$$

where $c_{k,l} = \sum_{j=0}^{M-1} H_l(\alpha_j)\overline{H_k(\alpha_j)}$. Also, we compute,

$$\mathbb{H}^*\widehat{\mathbb{F}} = \begin{pmatrix} \sum_{j=0}^{M-1} \overline{H_0(\alpha_j)}\widehat{f}(\alpha_j) \\ \vdots \\ \sum_{j=0}^{M-1} \overline{H_{N^2-1}(\alpha_j)}\widehat{f}(\alpha_j) \end{pmatrix}.$$

Consequently, we have

$$\begin{aligned} f_{\text{recon}} &= (\mathbb{H}^*\mathbb{H})^{-1}\mathbb{H}^*\widehat{\mathbb{F}} \\ &= \begin{pmatrix} \frac{1}{M}\sum_{j=0}^{M-1} H_0(\alpha_j)\overline{H_0(\alpha_j)} & \cdots & \frac{1}{M}\sum_{j=0}^{M-1} H_{N^2-1}(\alpha_j)\overline{H_0(\alpha_j)} \\ \vdots & & \vdots \\ \frac{1}{M}\sum_{j=0}^{M-1} H_0(\alpha_j)\overline{H_{N^2-1}(\alpha_j)} & \cdots & \frac{1}{M}\sum_{j=0}^{M-1} H_{N^2-1}(\alpha_j)\overline{H_{N^2-1}(\alpha_j)} \end{pmatrix}^{-1} \\ &\qquad \times \begin{pmatrix} \frac{1}{M}\sum_{j=0}^{M-1} \overline{H_0(\alpha_j)}\widehat{f}(\alpha_j) \\ \vdots \\ \frac{1}{M}\sum_{j=0}^{M-1} \overline{H_{N^2-1}(\alpha_j)}\widehat{f}(\alpha_j) \end{pmatrix}, \end{aligned}$$

which tends to

$$\begin{pmatrix} \int_{\left[\frac{K}{2},\frac{K}{2}\right]^2} H_0(\lambda)\overline{H_0(\lambda)}d\lambda & \cdots & \int_{\left[\frac{K}{2},\frac{K}{2}\right]^2} H_{N^2-1}(\lambda)\overline{H_0(\lambda)}d\lambda \\ \vdots & & \vdots \\ \int_{\left[\frac{K}{2},\frac{K}{2}\right]^2} H_0(\lambda)\overline{H_{N^2-1}(\lambda)}d\lambda & \cdots & \int_{\left[\frac{K}{2},\frac{K}{2}\right]^2} H_{N^2-1}(\lambda)\overline{H_{N^2-1}(\lambda)}d\lambda \end{pmatrix}^{-1}$$

$$\times \begin{pmatrix} \int_{\left[\frac{K}{2},\frac{K}{2}\right]^2} \overline{H_0(\lambda)}\widehat{f}(\lambda)d\lambda \\ \vdots \\ \int_{\left[\frac{K}{2},\frac{K}{2}\right]^2} \overline{H_{N^2-1}(\lambda)}\widehat{f}(\lambda)d\lambda \end{pmatrix},$$

as $M \to \infty$ and for $K >> 0$. This last matrix product is *approximately*

$$\begin{pmatrix} \langle H_0, H_0\rangle & \cdots & \langle H_{N^2-1}, H_0\rangle \\ \vdots & & \vdots \\ \langle H_0, H_{N^2-1}\rangle & \cdots & \langle H_{N^2-1}, H_{N^2-1}\rangle \end{pmatrix}^{-1} \begin{pmatrix} \langle \widehat{f}, H_0\rangle \\ \vdots \\ \langle \widehat{f}, H_{N^2-1}\rangle \end{pmatrix}$$

$$= \begin{pmatrix} |D_0| & & & 0 \\ & |D_1| & & \\ & & \ddots & \\ 0 & & & |D_{N^2-1}| \end{pmatrix}^{-1} \begin{pmatrix} \langle f, \mathbb{1}_{D_0} \rangle \\ \langle f, \mathbb{1}_{D_1} \rangle \\ \vdots \\ \langle f, \mathbb{1}_{D_{N^2-1}} \rangle \end{pmatrix}$$

$$= \begin{pmatrix} \frac{1}{|D_0|} \langle f, \mathbb{1}_{D_0} \rangle \\ \vdots \\ \frac{1}{|D_{N^2-1}|} \langle f, \mathbb{1}_{D_{N^2-1}} \rangle \end{pmatrix} = \begin{pmatrix} \frac{1}{|D_0|} \int_{D_0} f(x,y)dxdy \\ \vdots \\ \frac{1}{|D_{N^2-1}|} \int_{D_{N^2-1}} f(x,y)dxdy \end{pmatrix},$$

where we use Equation (19) and Parseval's theorem for the first equality.

Therefore, for a given $f \in L^2_N(D)$, we have

$$f_{\text{recon}} = (\mathbb{H}^*\mathbb{H})^{-1}\mathbb{H}^*\widehat{\mathbb{F}} \approx \left(\frac{1}{|D_0|} \int_{D_0} f(x,y)dxdy, \ldots, \frac{1}{|D_{N^2-1}|} \int_{D_{N^2-1}} f(x,y)dxdy \right)^T,$$

as asserted.

Remark 5. The above approximation of integrals by sums can be justified using results from the theory of uniformly distributed sequences, especially Theorem 5.5 (the Koksma-Hlawka inequality) and Theorem 6.1 and related techniques dealing with the discrepancy of sequences [40], Chapter 2. These methods are important with regard to exact frames, see [3], [49]. Further, continuity properties of matrix inversion enable the interchange of limits with matrix inverses in the calculation.

6. Computational aspects of the algorithm

6.1. **Computational feasibility.** To solve the basic problem of Section 4, i.e., reconstructing $f \in L^2_N(D)$ through

$$\widehat{\mathbb{F}} = \mathbb{H}\mathbb{F}, \tag{21}$$

and develop the associated algorithm formula, Equation (13), as we did in Subsection 4.1, we begin by addressing the system,

$$(\mathbb{H}^*\mathbb{H})\mathbb{F} = \mathbb{H}^*\widehat{\mathbb{F}}. \tag{22}$$

The dimensions of the vectors and matrices are:

- $\mathbb{F}$ is $N^2 \times 1$
- $\mathbb{H}$ is $M \times N^2$, where $M \geq N^2$
- $A = \mathbb{H}^*\mathbb{H}$ is $N^2 \times N^2$
- $\widehat{\mathbb{F}}$ is $M \times 1$
- $b = \mathbb{H}^*\widehat{\mathbb{F}}$ is $N^2 \times 1$.

Therefore, a direct implementation requires *memory* for

$$N^4 + (M+1)\,N^2 + M \geq 2\,(N^4 + N^2)$$

scalars. With regard to *operation count*, we have the following situation. The computations to solve Equation 22, assuming that $\mathbb{H}^*$ and $\mathbb{H}^*\mathbb{H}$ are given to us, involve computing $\mathbb{H}^*\widehat{\mathbb{F}}$ and $(\mathbb{H}^*\mathbb{H})^{-1}(\mathbb{H}^*\widehat{\mathbb{F}})$. The first term requires $O(M\,N^2)$ operations and the second term requires $O((N^2)^3)$ operations.

6.2. **Transpose reduction.** Set

$$\mathbb{H} = \begin{pmatrix} H_0(\alpha_0) & \dots & H_{N^2-1}(\alpha_0) \\ H_0(\alpha_1) & \dots & H_{N^2-1}(\alpha_1) \\ \vdots & & \vdots \\ H_0(\alpha_{M-1}) & \dots & H_{N^2-1}(\alpha_{M-1}) \end{pmatrix} = \begin{pmatrix} V_0^{\mathrm{T}} \\ V_1^{\mathrm{T}} \\ \vdots \\ V_{M-1}^{\mathrm{T}} \end{pmatrix},$$

where each V_j is $N^2 \times 1$, and $V_j = (H_0(\alpha_j), \dots, H_{N^2-1}(\alpha_j))^{\mathrm{T}}$. We compute

$$\begin{aligned}\mathbb{H}^*\mathbb{H} &= \begin{pmatrix} \sum_{k=0}^{M-1} \overline{H_0(\alpha_k)} H_0(\alpha_k), \dots, \sum_{k=0}^{M-1} \overline{H_0(\alpha_k)} H_{N^2-1}(\alpha_k) \\ \vdots \\ \sum_{k=0}^{M-1} \overline{H_{N^2-1}(\alpha_k)} H_0(\alpha_k), \dots, \sum_{k=0}^{M-1} \overline{H_{N^2-1}(\alpha_k)} H_{N^2-1}(\alpha_k) \end{pmatrix}, \\ &= \sum_{k=0}^{M-1} \begin{pmatrix} \overline{H_0(\alpha_k)} H_0(\alpha_k), \dots, \overline{H_0(\alpha_k)} H_{N^2-1}(\alpha_k) \\ \vdots \\ \overline{H_{N^2-1}(\alpha_k)} H_0(\alpha_k), \dots, \overline{H_{N^2-1}(\alpha_k)} H_{N^2-1}(\alpha_k) \end{pmatrix}, \\ &= \sum_{k=0}^{M-1} \begin{pmatrix} \overline{H_0(\alpha_k)} \\ \overline{H_1(\alpha_k)} \\ \vdots \\ \overline{H_{N^2-1}(\alpha_k)} \end{pmatrix} (H_0(\alpha_k), H_1(\alpha_k), \dots, H_{N^2-1}(\alpha_k)), \\ &= \sum_{k=0}^{M-1} \overline{V_k} V_k^{\mathrm{T}}. \end{aligned}$$

Also, we have

$$\mathbb{H}^*\widehat{\mathbb{F}} = \begin{pmatrix} \sum_{k=0}^{M-1} \overline{H_0(\alpha_k)} \widehat{f}_k \\ \vdots \\ \sum_{k=0}^{M-1} \overline{H_{N^2-1}(\alpha_k)} \widehat{f}_k \end{pmatrix} = \sum_{k=0}^{M-1} \widehat{f}_k \overline{V_k}.$$

Consequently, our algorithm for calculating $\mathbb{H}^*\mathbb{H}$ and $\mathbb{H}^*\widehat{f}$ requires the variables $A, V, \widehat{\mathbb{F}}$, and b. The algorithm is constructed as follows. Given $\{\alpha_0, \cdots, \alpha_{M-1}\}$ and $\widehat{\mathbb{F}} = (\widehat{f}_0, \dots, \widehat{f}_{M-1})^{\mathrm{T}}$.

(1) Let $V = [H_0(\alpha_0), \dots, H_{N^2-1}(\alpha_0)]^{\mathrm{T}}$, where a "for loop" of length N^2 is required to compute V;
(2) Define $A = \overline{V} V^{\mathrm{T}}$;
(3) Define $b = \widehat{f}_0 \overline{V}$;
(4) For $j = 1$ to $M-1$,
   - Let $V = [H_0(\alpha_j), \dots, H_{N^2-1}(\alpha_j)]^{\mathrm{T}}$;
   - Let $A = A + \overline{V} V^{\mathrm{T}}$;
   - $b = b + \widehat{f}_j \overline{V}$.

   end

Therefore, the algorithm requires memory for $N^2 \times N^2 + 2\,(M \times 1) + N^2 \times 1 + N^2 \times 1$ scalars. This is better than the direct implementation Equation (21) of Subsection 6.1.

The computational cost requires:

- $O(MN^2)$ calculations to compute the V vectors,
- $O(MN^4)$ calculations to compute $A = \mathbb{H}^*\mathbb{H}$, and

- $O(MN^2)$ calculations to compute $b = \mathbb{H}^*\widehat{\mathbb{F}}$.

Remark 6. The direct implementation uses more memory than the transpose reduction algorithm by a factor of roughly $(M/N^2) + 1$.

6.3. **An alternative.** As before, we begin with the system,

$$\mathbb{H}^*\mathbb{H}\mathbb{F} = \mathbb{H}^*\widehat{\mathbb{F}},$$

where $\mathbb{H}^*\mathbb{H}$ is of size $N^2 \times N^2$.

A problem arises from the fact that we have to build an $N^2 \times N^2$ matrix, when in fact we only need a set of N^2 coefficients to describe the image that we want to reconstruct from the frequency information contained in $\widehat{\mathbb{F}}$.

Let us review the process:

The unit square D is divided in N^2 smaller elements, in a grid-like fashion; and, as such, we deal with the characteristic functions for each of the $\left[\frac{k}{N}, \frac{k+1}{N}\right) \times \left[\frac{l}{N}, \frac{l+1}{N}\right)$ sub-squares.

Thus, an N-digital image $f \in L^2_N(D)$ is defined as

$$\sum_{k=0,l=0}^{N-1} f_{k,l} \mathbb{1}_{\left[\frac{k}{N}, \frac{k+1}{N}\right) \times \left[\frac{l}{N}, \frac{l+1}{N}\right)}.$$

When we have $M = N^2$ values of $\widehat{f}$, we are dealing with the exact and unique solution of $\mathbb{H}^*\mathbb{H}\mathbb{F} = \mathbb{H}^*\widehat{\mathbb{F}}$. When we have more than N^2 values of $\widehat{f}$, i.e., when $M > N^2$, then we are dealing with a *minimum squares solution.*

It is natural to ask how one can formulate this situation in terms of some *energy.* Consider the function,

$$E(\mathbf{v})(\lambda, \mu) = \sum_{i=0}^{N^2-1} v_i \widehat{\mathbb{1}}_i(\lambda, \mu),$$

where $\mathbf{v} = (v_0, \ldots, v_{N^2-1})^{\mathrm{T}} \in \mathbb{R}^{N^2}$ and

$$\mathbb{1}_i = \mathbb{1}_{\left[\frac{k_i}{N}, \frac{k_i+1}{N}\right) \times \left[\frac{l_i}{N}, \frac{l_i+1}{N}\right)},$$

for $0 \leq k_i, l_i \leq N - 1$.

Also, consider the data set $\{\widehat{f}_j = \widehat{f}(\lambda_j, \mu_j) : (\lambda_j, \mu_j) \in \widehat{\mathbb{R}}^2,\ 0 \leq j \leq M-1\}$, where $\widehat{f}$ is the Fourier transform of $f : \mathbb{R}^2 \to \mathbb{R}$.

We build the function $\mathcal{F} : \mathbb{R}^{N^2} \longrightarrow \mathbb{R}$ as follows:

$$\mathcal{F}(\mathbf{v}) = \sum_{j=0}^{M-1} \left| \sum_{i=0}^{N^2-1} v_i \widehat{\mathbb{1}}_i(\lambda_j, \mu_j) - \widehat{f}_j \right|^2 = \sum_{j=0}^{M-1} \left| E(\mathbf{v})(\lambda_j, \mu_j) - \widehat{f}_j \right|^2.$$

We want to find $\mathbf{v}_* \in \mathbb{R}^{N^2}$ such that

$$\mathcal{F}(\mathbf{v}_*) = \min_{\mathbf{v} \in \mathbb{R}^{N^2}} \mathcal{F}(\mathbf{v}).$$

We shall take the following course of action. First, the minimization approach will not be pursued because of the calculation of $\mathcal{F}(\mathbf{v})$ is generally too expensive. In fact, we shall take the *conjugate gradient approach* to solving the system,

$$\mathbb{H}^*\mathbb{H}\mathbb{F} = \mathbb{H}^*\widehat{\mathbb{F}}. \tag{23}$$

It makes sense to take this approach for the following reasons.

(1) Modulo the problem of storing $\mathbb{H}$, we can solve in a finite number of steps equation (23) perfectly, if perfect arithmetic, as opposed to other iterative methods.
(2) Since the storage of $\mathbb{H}$ is prohibitively expensive, we shall have to resort to computing $\mathbb{H}^*\mathbb{H}p_k$ iteratively, where p_k is from the usual conjugate gradient algorithm notation. Note that $\mathbb{H}^*\mathbb{H}$ is implicitly stored that way.
(3) The storage requirements are reduced to 4 vectors, in our case, of size $N^2 \times 1$. In reality we need an extra vector that grows as $M \times 1$ to be able to compute $\mathbb{H}^*\mathbb{H}p_k$.

This method makes sense when $\mathbb{H}^*\mathbb{H}$ is positive-definite.

For perspective, the Kaczmarz algorithm is a different approach to signal reconstruction that can operate with low memory requirements by using simple row-action updates, e.g., [16]. The Kaczmarz algorithm has figured prominently in computerized tomography.

7. An MRI primer

The ideas behind the discovery of *magnetic resonance imaging*, are due to Paul Lauterbur, see [21]. We outline and illustrate them.

A *magnetic dipole* is a spinning charged particle. A magnetic dipole has a *magnetic dipole moment* that is characterized by its *gyromagnetic ratio* γ and its *spin angular momentum* $\mathbf{S}$. We call this magnetic dipole moment μ, and $\mu = \gamma\mathbf{S}$, [31]. See Figure 2.

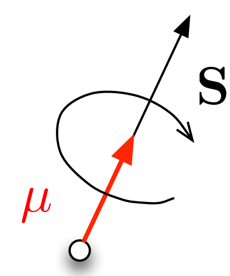

Figure 2. A *magnetic dipole* is a spinning charged particle.

If we place a magnetic dipole in the presence of a static magnetic field $\mathbf{B}_0$, and its magnetic dipole moment is not aligned with the magnetic field, we observe that the magnetic dipole moment precesses about the magnetic field at a frequency ω_0 called the *Larmor frequency*. The Larmor frequency is proportional to the strength of the magnetic field. The constant of proportionality is the gyromagnetic ratio, i.e., $\omega_0 = \gamma\|\mathbf{B}_0\|_2$, [31], [41]. See Figure 3.

If a macroscopic sample of magnetic dipoles in solid, liquid, or gaseous form (for example, about 10^{23} hydrogen nuclei in water per cm^3) is placed in the presence of a static magnetic field $\mathbf{B}_0$, then the energy in this sample will be minimized when the majority of the magnetic dipole moments align with $\mathbf{B}_0$. This minimum energy state gives rise to a local *magnetization* M of the sample, and $M = \chi\mathbf{B}_0$, where χ is called the *nuclear susceptibility* of the sample, [41]. See Figure 4.

Suppose that we place a circular coil centered on a macroscopic sample of magnetic dipoles that has been magnetized by a static magnetic field $\mathbf{B}_0$, and suppose that the coil is embedded in a plane containing $\mathbf{B}_0$. See Figure 5. We then apply a time varying sinusoidal voltage $v(t) = A\sin(\omega t)$ at the coil with amplitude A and frequency ω. We observe a time

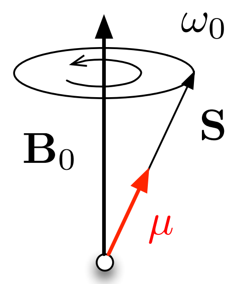

FIGURE 3. Magnetic dipole precession in the presence of a magnetic field.

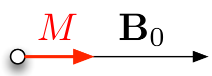

FIGURE 4. Magnetization of a macroscopic sample of magnetic dipoles.

varying magnetic field $\mathbf{B}_1(t)$ perpendicular to $\mathbf{B}_0$ that will grow and shrink, coming in and out of the plane containing the coil.

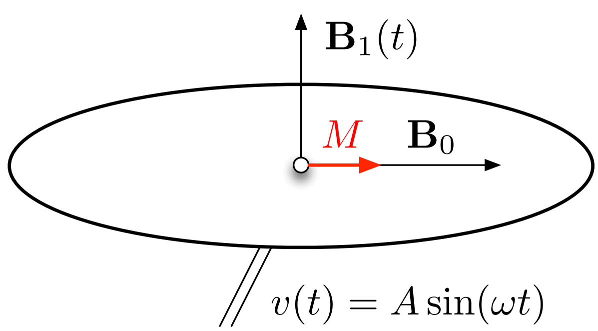

FIGURE 5. Magnetization of a sample and coil experiment.

The *nuclear magnetic resonance* or NMR phenomenon can then be observed at the Larmor voltage frequency ω_0 in the following way: the magnetization in the sample is rotated and placed in the transversal plane to $\mathbf{B}_0$, [31], [41]. See Figure 6.

When the voltage pulse that generated the magnetic field $\mathbf{B}_1$ is turned off, we then observe an induced voltage $S(t)$ in the coil as the magnetization of the sample M precesses around $\mathbf{B}_0$ eventually aligning with it. This relaxation process is triggered by thermal noise in the sample, [41]. See Figure 7.

The magnetization M can be decomposed in longitudinal and transversal components, M_{lon} and M_{tr}, respectively. The longitudinal component will be parallel to $\mathbf{B}_0$ and the transversal component will be in the transversal plane perpendicular to $\mathbf{B}_0$, [41]. See Figure 8.

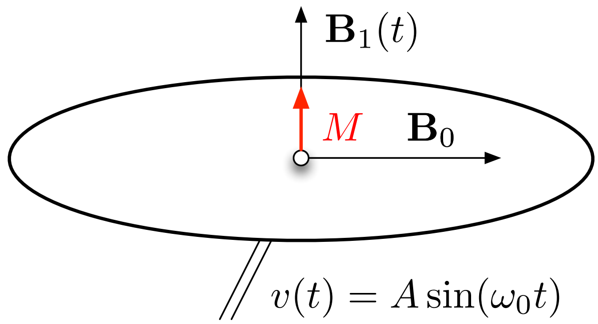

FIGURE 6. Nuclear magnetic resonance (NMR) observed at the Larmor frequency.

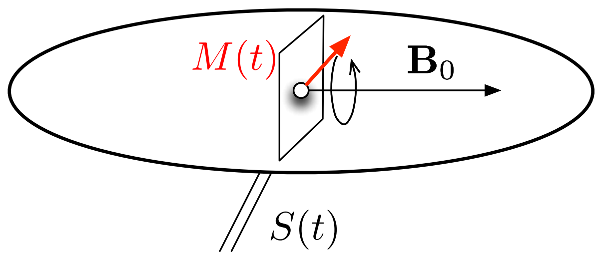

FIGURE 7. Relaxation of the magnetization of a sample to its steady state.

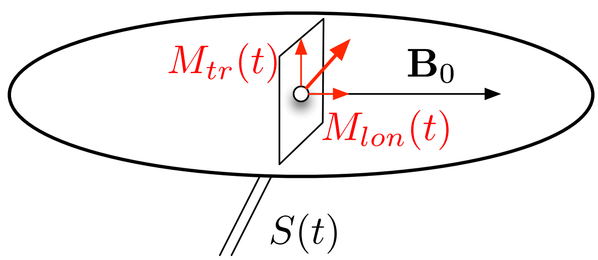

FIGURE 8. Transversal and longitudinal magnetizations.

Bloch's equations predict in a variety of cases that the decay to the steady state of the magnetization will be exponential, i.e.,

$$M_{lon} - \chi \mathbf{B}_0 \propto \exp(-t/T_1), \tag{24}$$

$$\|M_{tr}\|_2 \propto \exp(-t/T_2), \tag{25}$$

where $\propto$ denotes *proportional to* and where the characteristic relaxation times T_1 and T_2 are particular to the magnetization sample, [41].

With this physical setup, we arrive at the imaging equation, Equation (1), of Section 2, viz.,

$$\begin{aligned} S(t) &= S(k(t)) = S(k_x(t), k_y(t), k_z(t)) \\ &= \int\int\int M_{tr}(x,y,z) e^{-2\pi i \langle (x,y,z),(k_x,k_y,k_z)\rangle} dx\, dy\, dz \\ &= \int\int\int \rho(x,y,z) e^{-t/T_2} e^{-2\pi i \langle (x,y,z),(k_x,k_y,k_z)\rangle} dx\, dy\, dz, \end{aligned} \tag{26}$$

where we have introduced the transversal component M_{tr}, where ρ is a magnetic dipole density function of space, where $\mathbf{r} = (x,y,z)$, and where $k_s(t)$ for $s = x,y,z$ is proportional to

$$\int_0^t \frac{\partial}{\partial s} \mathbf{B}_0(u) du, \tag{27}$$

cf. Equation (2) of Section 2. Thus, the induced signal S can be seen as the Fourier transform of the transversal magnetization M_{tr} in the k-spectral domain. Hence, to recover the transversal magnetization we take the inverse Fourier transform of the signal S. The transversal magnetization $M_{tr} = M_{tr}(\mathbf{r},t) = \rho(\mathbf{r})e^{-t/T_2}$ is also a function of time t, as seen in Equation (26). In practice, the values of k_r in the k-spectral domain are obtained by sampling (27) at regular time intervals. For this strategy to work, the magnetic field $\mathbf{B}_0$ must have a non-zero gradient. Hence, the design of magnetic gradients plays an important role in the sampling strategy of the k-spectral domain from which we recover an image in the spatial domain of M_{tr}, and from which we obtain an image of the density ρ, [41].

8. Synthetic data generation

We give the logic for the empirical evaluation of the algorithm in the case when data is not machine provided automatically, e.g., from an actual MRI.

- Given a high resolution image I (1024×1024).
- Downsample I (e.g., by taking averages) to I_N, $N \times N$, where, for example, N could be 128 or 256.
- Therefore, for comparison purposes, I_N is the optimal, *available* image at the $N \times N$ level.
- Calculate $\widehat{I} = \sum I_{a_k} H_{a_k}$, i.e., 10^6 terms for each $\alpha_m \in \widehat{\mathbb{R}}^2$.
- Choose $\widehat{I}(\alpha_m)$, $m = 0, 1, \ldots, M-1 \geq N^2 - 1$, appropriately, where the α_m are on a finite union of sufficiently tightly wound Archimedean spirals, for example, and are restricted to a $[K,K]^2$ square.
- Set $LI = \widehat{I}$, an $M \times 1$ vector.
- Implementation gives

  $$\tilde{I} = S^{-1} L^* \widehat{I},$$

  that has matrix dimension,

  $$(N^2 \times N^2)(N^2 \times M)(M \times 1) = N^2 \times 1.$$

- Quantitatively analyze the difference $I_N - \tilde{I}$, an $N \times N$ matrix.

References

[1] C. B. Ahn, J. M. Kim, and Z. H. Cho. High speed spiral-scan echo planar NMR imaging - I. *IEEE Transactions on Medical Imaging*, 5:2–7, 1986.

[2] Ovidiu C. Andronesi, Borjan A. Gagoski, and A. Gregory Sorensen. Neurologic 3D MR spectroscopic imaging with low-power adiabatic pulses and fast spiral acquisition. *Radiology*, 262 (2):647–661, 2012.

[3] S. A. Avdonin. On the question of Riesz bases of complex exponential functions in l^2. *Vestnik Leningrad Univ. Ser. Mat. (Vestnik Leningrad Univ. Ser. Math., English translation)*, 13 (7):5–12 (1979), 1974 (1979).

[4] John J. Benedetto. Frame decompositions, sampling, and uncertainty principle inequalities. In John J. Benedetto and Michael W. Frazier, editors, *Wavelets: Mathematics and Applications*, pages 247–304. CRC Press, Boca Raton, FL, 1994.

[5] John J. Benedetto. Noise reduction in terms of the theory of frames. In *Signal and Image Representation in Combined Spaces, J. Zeevi and R. Coifman, editors*, pages 259–284, invited. Academic Press, New York, 1998.

[6] John J. Benedetto, Alfredo Nava-Tudela, Alexander M. Powell, and Yang Wang. Finite frame implementation for spiral-scan echo planar MRI. *Technical Report*, 2002.

[7] John J. Benedetto and Anthony Teolis. A wavelet auditory model and data compression. *Applied and Computational Harmonic Analysis*, 1:3–28, 1993.

[8] John J. Benedetto and Anthony Teolis. Local frames and noise reduction. *Signal Processing*, 45:369–387, 1995.

[9] John J. Benedetto and David Walnut. Gabor frames for L^2 and related spaces. *Wavelets: Mathematics and Applications, edited by J.J. Benedetto and M. Frazier, CRC*, pages 97–162, 1994.

[10] John J. Benedetto and Hui-Chuan Wu. A Beurling covering theorem and multidimensional irregular sampling. In *SampTA*, Loen, 1999.

[11] John J. Benedetto and Hui-Chuan Wu. A multidimensional irregular sampling algorithm and applications. *IEEE-ICASSP*, 1999.

[12] John J. Benedetto and Hui-Chuan Wu. Non-uniform sampling and spiral MRI reconstruction. *SPIE*, 2000.

[13] Arne Beurling. Local harmonic analysis with some applications to differential operators. *Some Recent Advances in the Basic Sciences, Vol. 1 (Proc. Annual Sci. Conf., Belfer Grad. School Sci., Yeshiva Univ., New York, 1962–1964)*, pages 109–125, 1966.

[14] Marc Bourgeois, Frank T.A.W. Wajer, Dirk van Ormondt, and Danielle Graveron-Demilly. Reconstruction of MRI images from non-uniform sampling and its application to intrascan motion correction in functional MRI. In John J. Benedetto and Paulo J. S. G. Ferreira, editors, *Modern Sampling Theory; Mathematics and Applications*, pages 343–363. Birkäuser, Boston, 2001.

[15] Peter G. Casazza and Gitta Kutyniok. *Finite Frames: Theory and Applications.* Applied and Numerical Harmonic Analysis. Birkhäuser Boston, 2012.

[16] Xuemei Chen and Alexander M. Powell. Almost sure convergence of the Kaczmarz algorithm with random measurements. *Journal of Fourier Analysis and Applications*, 18:1195–1214, 2012.

[17] Z.-H. Cho, O. Nalcioglu, and H. W. Park. Methods and algorithms for Fourier transform nuclear magnetic resonance tomography. *Journal of the Optical Society of America*, 4:923–932, 1987.

[18] Zang-Hee Cho, Joie P. Jones, and Manbir Singh. *Foundations of Medical Imaging.* Wiley-Interscience, New York, 1993.

[19] Ole Christensen. *An Introduction to Frames and Riesz Bases, 2nd edition.* Springer-Birkhäuser, New York, 2016 (2003).

[20] Ingrid Daubechies. *Ten Lectures on Wavelets.* Society for Industrial and Applied Mathematics, Philadelphia, PA, 1992.

[21] M. Joan Dawson. *Paul Lauterbur and the invention of MRI.* The MIT Press, 2013.

[22] J. F. Debatin and G. C. McKinnon. *Ultrafast MRI.* Springer, New York, 1998.

[23] Bénédicte M.A. Delattre, Robin M. Heidemann, Lindsey A. Crowe, Jean Paul Valle, and Jean Noël Hyacinthe. Spiral demystified. *Magnetic Resonance Imaging*, 28 (6):862–881, 2010.

[24] Richard James Duffin and Albert Charles Schaeffer. A class of nonharmonic Fourier series. *Transactions of the American Mathematical Society*, 72:341–366, 1952.

[25] A. Dutt and V. Rokhlin. Fast Fourier transforms for nonequispaced data, II. *Applied and Computational Harmonic Analysis*, 2(1):85–100, 1995.

[26] Karsten Fourmont. Nonequispaced fast Fourier transforms with applications in tomography. *Journal of Fourier Analysis and Applications*, 9(5):431–450, 2003.

[27] Jean-Pierre Gabardo. Weighted tight frames of exponentials on a finite interval. *Monatshefte für Mathematik*, 116:197–229, 1993.

[28] Gary H. Glover and Adrian T. Lee. Motion artifacts in FMRI: Comparison of 2DFT with PR and spiral scan methods. *Magnetic Resonance in Medicine*, 33:624–635, 1995.

[29] Gary H. Glover and John M. Pauly. Projection reconstruction techniques for reduction of motion effects in MRI. *Magnetic Resonance in Medicine*, 28:275–289, 1992.

[30] Leslie Greengard and June Yub Lee. Accelerating the nonuniform fast Fourier transform. *SIAM Review*, 46(3):443–454, 2004.

[31] David J. Griffiths. *Introduction to Quantum Mechanics*. Pearson Prentice Hall, 2nd edition, 2005.

[32] Ray H. Hashemi and William G. Bradley. *MRI: the Basics*. Williams and Wilkins, a Waverly Company, Baltimore, 1997.

[33] Dennis M. Healy Jr. and John B. Weaver. Two applications of wavelet transforms in magnetic resonance imaging. *IEEE-Transactions on Information Theory*, 38(2):840–860, March 1992.

[34] Josef Hofbauer. A simple proof of $1 + 1/2^2 + 1/3^2 + \cdots = \pi^2/6$ and related identities. *Amer. Math. Monthly*, 109(2):196–200, 2002.

[35] Richard D. Hoge, Remi K. S. Kwan, and G. Bruce Pike. Density compensation functions for spiral MRI. *Magnetic Resonance in Medicine*, 38(1):117–128, 1997.

[36] M. I. Kadec. Bases and their spaces of coefficients. *Dopov. Akad. Ukr. RSR*, 9:1139–1141, 1964.

[37] Jens Keiner, Stefan Kunis, and Daniel Potts. Using NFFT 3—a software library for various nonequispaced fast Fourier transforms. *Journal ACM Transactions on Mathematical Software*, 36(4), 2009.

[38] J. Kovačević and A. Chebira. Life beyond bases: The advent of frames (part I). *Signal Processing Magazine, IEEE*, 24(4):86–104, 2007.

[39] J. Kovačević and A. Chebira. Life beyond bases: The advent of frames (part II). *Signal Processing Magazine, IEEE*, 24:115–125, 2007.

[40] L. Kuipers and H. Niederreiter. *Uniform Distribution of Sequences*. Wiley-Interscience [John Wiley & Sons], New York, 1974.

[41] Vadim Kuperman. *Magnetic Resonance Imaging. Physical Principles and Applications*. Academic Press, 2000.

[42] Henry J. Landau. Necessary density conditions for sampling and interpolation of certain entire functions. *Acta Mathematica*, 117:37–52, 1967.

[43] Jan Ray Liao, John M. Pauly, and Norbert J. Pelc. MRI using piecewise-linear spiral trajectory. *Magnetic Resonance in Medicine*, 38:246–252, 1997.

[44] Stig Ljunggren. A simple graphical representation of Fourier based imaging method. *Journal of Magnetic Resonance*, 54:338–343, 1983.

[45] Michael Lustig, David Donoho, and John M. Pauly. Sparse MRI: the application of compressed sensing to rapid MR imaging. *Magnetic Resonance in Medicine*, 58:1182–1195, 2007.

[46] Alexander M. Powell. Lattice points on interleaving spirals. *Technical Note*, 2016.

[47] Alexander M. Powell, Jared Tanner, Yang Wang, and Özgur Yılmaz. Coarse quantization for random interleaved sampling of bandlimited signals. *ESAIM Mathematical Modelling and Numerical Analysis*, 46:605–618, 2012.

[48] Walter J. Rudin. *Functional Analysis*. McGraw-Hill, New York, 1991.

[49] Kristian Seip. A simple construction of exponential bases in l^2 of the union of several intervals. *Proc. Edinburgh Math. Society*, 38(1):171–177, 1995.

[50] Andreas Sigfridsson, Sven Petersson, Carl-Johan Carlhäll, and Tino Ebbers. Four-dimensional flow MRI using spiral acquisition. *Magnetic Resonance in Medicine*, 68 (4):1065–1073, 2012.

[51] Wenchang Sun and Xingwei Zhou. On the stability of multivariate trigonometric systems. *Journal of Mathematical Analysis and Applications*, 235:159–167, 1999.

[52] Robert M. Young. *An Introduction to Nonharmonic Fourier Series*. Academic Press, New York, 1980.

[1]Norbert Wiener Center, Department of Mathematics, University of Maryland, College Park, MD 20742, USA
E-mail address: jjb@math.umd.edu

[2]Institute for Physical Science and Technology, University of Maryland, College Park, MD 20742, USA
E-mail address: ant@umd.edu

[3]Department of Mathematics, Vanderbilt University, Nashville, TN 37240, USA
E-mail address: alexander.m.powell@vanderbilt.edu

[4]Department of Mathematics, The Hong University of Science and Technology, Clear Water Bay, Kowloon, Hong Kong
E-mail address: yangwang@ust.hk